Sensors and Actuators B 268 (2018) 29–38

Contents lists available at ScienceDirect

Sensors and Actuators B: Chemical

journal homepage: www.elsevier.com/locate/snb

Benzothiazole based Schiff-base-A mechanistically discrete sensor for HSO_4^- and I^-: Application to bioimaging and vapour phase sensing of ethyl acetate

Ishpreet Kaur[a], Anjali Khajuria[b], Puja Ohri[b], Paramjit Kaur[a,*], Kamaljit Singh[a,*]

[a] Department of Chemistry, UGC-Centre of Advanced Study-II, Guru Nanak Dev University, Amritsar, 143005, India
[b] Department of Zoology, Guru Nanak Dev University, Amritsar, 143005, India

ARTICLE INFO

Article history:
Received 1 February 2018
Received in revised form 12 April 2018
Accepted 13 April 2018
Available online 18 April 2018

Keywords:
Schiff-base
HSO_4^- and I^- ions
TD-DFT
Molecular electrostatic potential map
Nematodes
Vapours of ethyl acetate

ABSTRACT

We report a 2-(4-amino-2-hydroxyphenyl)benzothiazole based Schiff-base, found to be sensitive to the presence of HSO_4^- and I^- ions as demonstrated by modulation of the various photophysical properties in the presence of these ions in solution and biological enviornments (nematodes). Various spectroscopic and TD-DFT calculations have revealed that while the molecular probe detects HSO_4^- ions *via* hydrolytic cleavage and subsequent emission enhanced mechanism, the detection of I^- ions is accomplished *via* the formation of intermolecular charge transfer complex and the subsequent heavy atom quenching mechanism. Additionally the potential of the probe for the on site detection of vapours of ethylacetate at workplaces has been demonstrated.

1. Introduction

In view of the significant role of anions in a wide range of chemical and biological processes, the design and synthesis of the probes capable of selective binding and sensing of anions has attracted much interest in the recent years [1]. The detection of oxoanions (derived from oxoacids through deprotonation), especially hydrogen sulphate (HSO_4^-) draws significance owing to its important role in biological endeavours and industrial sectors such as agricultural fertilisers, industrial raw materials, nuclear fuel wastes *etc* [2,3]. The presence of HSO_4^- or its dissociated by-product SO_4^{2-} as a pollutant in the environment poses severe health problems ranging from irritation in eyes and skin, and respiratory issues [4]. Meanwhile, iodide (I^-) constitutes an essential micronutrient, as it plays an important role in functioning of thyroid gland and neurological activity [5] in humans, and has thus its detection has attracted special interest over the other halides. According to World Health Organisation (WHO) estimates, both the deficiency and the excessive intake of iodide can lead to thyroid disorders and this has become a matter of considerable concern for public health in many countries [6]. Also the discharges from the industries associated with manufacture of pharmaceuticals, dyes and chemicals [7] *etc.* employing oxidised form of iodide (elemental iodine) in water bodies pose additional challenges. The lethal effects of both of these inorganic anions have thus necessitated the development of new molecular probes for their detection in environmental as well as biological samples. Working on the development of receptors for different analytes [8–11], we and other research groups have previously reported suitable probes for the detection of HSO_4^- and I^- ions [12–17]. The receptors for HSO_4^- ions, have relied on either hydrogen bonding (non Schiff-bases) [17–20] or reaction based (Schiff-bases) motifs, but are dominated by the former types [21–24]. Considering the pKa value of HSO_4^- (1.99 in aqueous medium), its behaviour as a H^+ donor is obligatory in aqueous/semi aqueous medium in stark contrast to the H^+ accepting basic anions such as I^-, Br^-, F^- *etc.* [25]. In recognition of the former, we envisioned sensitivity of the —CH=N link in the Schiff-base receptor **3** (Scheme 1), in the presence of protic anions in the aqueous hydrolytic media [22], as well as expected **3** to behave contrarily in the presence of basic anions. Indeed, probe **3** behaved as a chemodosimeter, wherein enhancement of fluorescence emission was noted in the presence of HSO_4^-, whereas **3** acted as a chemosensor and recognised I^- *via* emission quenching as depicted in Scheme 1. Consequently, differential modulation of the photophysical prop-

---

* Corresponding authors.
E-mail addresses: paramjit19in@yahoo.co.in (P. Kaur), kamaljit.chem@gndu.ac.in (K. Singh).

https://doi.org/10.1016/j.snb.2018.04.072

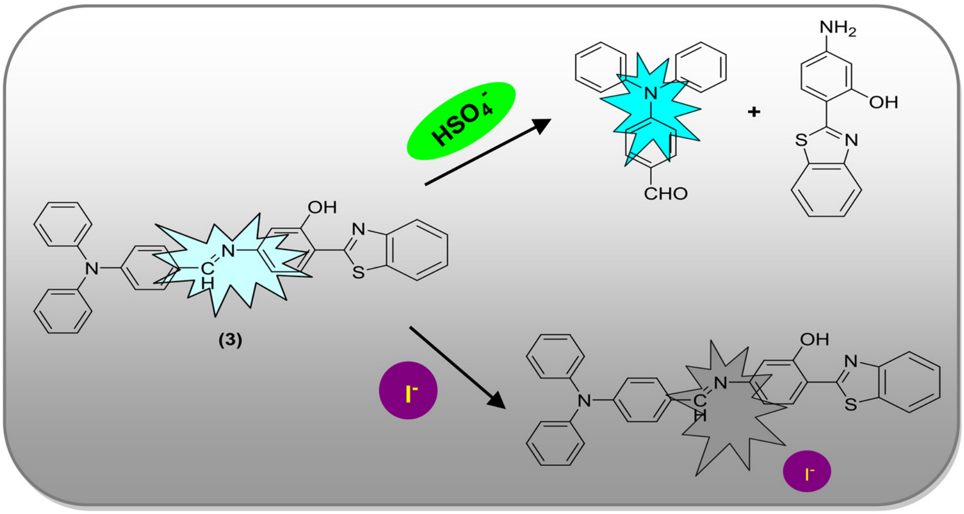

Scheme 1. The two way mechanistic approach adopted by **3** for the detection of HSO_4^- and I^- ions.

erties of **3** in the presence of HSO_4^- and I^- ions led to the detection, through discrete modes. The process has been further extended to the detection of these ions in the living nematodes, which in fact, constitutes the first example. Interestingly we also observed that the probe **3** is responsive towards ethyl acetate vapours.

2. Experimental

2.1. Materials and reagents

All liquid reagents were dried/purified using recommended drying agents and/or distilled over 4 Å molecular sieves. DMF and EtOH were stored overnight over molecular sieves. Other solvents (analytical grade) used for the analytical work were purchased from Thomas Baker, while the ones used for the synthetic work were of synthesis grade. The metal salts, 4-aminosalicylic acid and triphenylamine were purchased from Sigma–Aldrich and used as such. Stock solutions (0.1 M) of sodium salts of OH^-, Cl^-, Br^-, I^-, F^-, $H_2PO_4^-$, CN^-, CH_3COO^-, PO_4^{3-}, HSO_3^-, HSO_4^-, NO_3^-, ADP^{2-}, ATP^{2-}, CO_3^{2-}, SO_3^{2-} were prepared in double distilled water, whereas stock solution of **3** (1×10^{-3}M) was prepared in tetrahydrofuran (THF).

2.2. Instrumentation

IR spectra were recorded on Agilent Technologies Cary 630 FTIR spectrophotometer in the range 650–4000 cm^{-1}. Fluorescence studies were carried out using Perkin Elmer LS 55 Fluorescence Spectrometer, having a xenon flash lamp with pulse at a line frequency of 50–60 Hz. The fluorescence spectrometer consists of Monk-Gillieson type monochromators having range of excitation: 200–800 nm and emission: 200–900 nm with zero order R928 photomultiplier. The fluorescence spectroscopic studies were carried out using ultraviolet (UV) LED with excitation wavelength of 337 nm, focused perpendicularly to one side of the fluorescence quartz cuvette at excitation slit width of 15 nm. The emission spectrum was recorded by scanning the monochromator in the visible region from 350 to 650 nm using emission slit width of 5 nm and detecting the optical signal using a photomultiplier tube located at the exit port of the monochromator, which is further connected to a power meter. UV–vis studies were carried out using UV-1800 SHIMADZU UV-Spectrophotometer. The pH titrations were carried out using Equip-Tronics Digital pH meter model-EQ 610 and electrode was calibrated using standard buffers of pH 4.0, 7.0 and 9.2. ^1H NMR and ^{13}C NMR spectra were recorded on JEOL-FT NMR-AL at 300 MHz and Bruker Avance II NMR spectrometer at 400 MHz, with TMS as internal standard using $CDCl_3$, DMSO-d_6 and D_2O as deuterated solvent. Data are reported as follows: chemical shift in ppm (δ), integration, multiplicity (s = singlet, d = doublet, t = triplet, m = multiplet), coupling constant J (Hz) and assignment. The NMR titrations (^1H: 400 MHz) were performed on Bruker Avance II NMR spectrometer at 400 MHz. Mass spectrum (MS) was recorded on Bruker HRMS MICROTOF II spectrometer. Melting points were determined in open capillaries and are uncorrected.

2.3. Computational details

All theoretical calculations were performed by using Gaussian09 suite of programmes [26]. The molecular geometries of the chromophores were optimised at the density functional theory (DFT) method employing the hybrid B3LYP functional. 6-31G/3-21G Basis set were used for C, H, S, O, N, and I^- atoms. The same models were used for the calculation of the properties of the chromophores. The first 30 excited states were calculated by using time-dependent density functional theory (TD-DFT calculations). The molecular orbital contours were visualised using Gauss view 5.0.9.

2.4. Quantum yield calculations

The fluorescence quantum yields were measured using 9,10-diphenylanthracene as standard having quantum yield of 0.95 in cyclohexane [27], using the following equation:

$$\Phi_u = \frac{F_u(1 - 10^{-A_s\ L_s}) \times n_u^2}{F_s(1 - 10^{-A_u\ L_u}) \times n_s^2} \times \Phi_s$$

where Φ_u and Φ_s are the quantum yields of the test and the standard samples, respectively. A_u and A_s are the absorbance values of the test sample and the standard sample respectively, F_u and F_s are the areas of emission bands for the test sample and the standard sample, n_u and n_s are the refractive indices of test sample and standard sample solutions in their respective pure solvents. L is length of cell (1.0 cm for standard and test samples).

2.5. Detection limit Calculations

The detection limit (for I^-) was calculated on the basis of the fluorescence titration. The fluorescence emission spectrum of **3** was measured 6 times, and the standard deviation of blank mea-